EXPERIMENTAL CHARACTERIZATION OF THE ENTRAINED DROPLET VELOCITIES INTO A SUBMERGED GASEOUS JET

C. Berna[1]*, J. E. Juliá[2], A. Escrivá[1], J.L. Muñoz-Cobo[1] and J. V. Pastor[3].
*Author for correspondence
[1] Instituto de Ingeniería Energética
Universitat Politècnica de València (UPV)
Camino de Vera s/n, 46022 València (Spain)
Tel: 0034·963879245, Email: ceberes@iie.upv.es
[2] Department of Mechanical Engineering and Construction
Universitat Jaume I
Campus del Riu Sec s/n, 12071 Castelló de la Plana (Spain)
[3] CMT-Motores Térmicos
Universitat Politècnica de València (UPV)
Camino de Vera s/n, 46022 València (Spain)

ABSTRACT

The study of submerged gaseous jets injected into stagnant water pools began in the 70s caused by the fact that they are commonly found in many industrial processes and engineering applications, such as underwater propulsion, metallurgical and chemical processes or nuclear reactors. Consequently it is important to be able to characterize these processes.

The low air-water density ratio and the aggressiveness of the pool discharge process result in very complicated flow structures, which are inherently unsteady and turbulent. This poses a major challenge for the measurement of the various parameters involved in the discharge of gaseous submerged jets.

Experimental studies of round turbulent air jets submerged in stagnant water are described in this paper. In particular, the entrained droplet velocity, which is crucial for the characterization of the jet, was determined.

The experiments were performed using a water tank equipped with an air injector. A high speed camera in conjunction with Particle Image Velocimetry (PIV) techniques was used to measure the velocity of the entrained droplets during jet spreading.

Results indicate that the droplet velocity distribution follows a decreasing exponential function. Moreover, the Reynolds number at the injector nozzle was used to develop a correlation linking the initial jet properties and the mean velocity of the entrained droplets.

This work represents a new step towards a better understanding of the behavior of submerged gas jets injected into aqueous mediums. The velocity of the entrained droplets was determined, both its mean and distribution function. The extension of the present work to different nozzle diameters and aqueous mediums properties will be addressed in an upcoming paper.

NOMENCLATURE

c	[m/s]	Wave celerity
D	[m]	Jet diameter
p_0	[MPa]	Stagnation pressure
Re_d	[-]	Droplet Reynolds number
Re_g	[-]	Gas Reynolds number
Re_l	[-]	Liquid Reynolds number
S_R	[-]	Slip ratio
Stk	[-]	Stokes number
u_d	[m/s]	Entrained droplet velocity
u_g	[m/s]	Gas velocity
v_i	[m/s]	Central value of droplet velocity in each interval of the exponential distribution function
We_g	[-]	Gas Weber number

Special characters

ϕ_d	[m]	Droplet diameter
ψ	[-]	Adjustment parameter of Kumar's correlation
λ	[-]	Rate parameter of the exponential distribution function
μ	[Pa·s]	Dynamic viscosity
ρ	[kg/m^3]	Density
σ	[N/m]	Surface tension
τ	[-]	Dimensionless response time

Subscripts

0	Initial
d	Droplet
g	Gas
l	Liquid

INTRODUCTION

The study of submerged gas jets started in the 70s and 80s caused by increasing interests of nuclear industry (investigations related with fast breeder reactors) and the metallurgical industry, after this first impulse another strong push took place at the later part of the twentieth century from the advent of pharmaceutical industries, propulsion systems for underwater propulsion, chemical industries and also supported by the nuclear an metallurgical industries.

For instance, the importance of submerged gas jets in metallurgical industry is due to their wide use for liquid metal stirring and gas-metal reactions as the high velocity of gas jets enhance mixing efficiency through the high surface to volume ratio of the bubbly mixture. The submerged gas jet injection was extensively studied in this field from the 1970's, when the severe erosion of tuyere refractory was found in supplying oxygen gas into steelmaking furnaces [1].

Also from the 70s the submerged gas jet were widely studied, due to his importance in the design of safe steam generators for Fast Breeder Reactors (FBR), because of the importance to understand the reactions that occur between sodium and water (in a Steam Generator Tube Rupture event, highly pressurized water or steam escapes towards the surrounding liquid sodium) [2,3]. Also within the nuclear industry, the study of submerged gas jets is important for both BWR and PWR nuclear power plants. Pool scrubbing (discharge processes of nuclear aerosols in the suppression pool) has been traditionally associated with Beyond Design Limits of BWRs but may have importance in PWRs due to the open of direct transport paths for the fission products to the surrounding areas (SGTR events, discharge processes of nuclear aerosols in the secondary circuit). They Fukushima accident is another example of the importance of understanding the way in which submerged gas jets evolve.

Concentrating on gas jet characterization, two kinds of regimes can exit for the development of the submerged gas flow after leaving the nozzle exit. The bubbling regime exits for low flow rate conditions, this regime is characterized by the production of big bubbles that break near the nozzle and rise towards the free liquid surface. For higher gas flow rates the jet regime takes place, this regime remains relatively stable and only far downstream (several centimetres) of the nozzle exit break into bubbles and rises.

This paper focuses on the characterization of the entrained droplets velocity along the jet region. Its structure is as follows, in the first place, the presentation of previous expressions and correlations to determine the entrained droplet velocity profiles. After this first approach to the problem, the experimental facility, its instrumentation and the image capture and treatment are developed. After the facility description and experimental data treatment, the document continues with the main part of this work, the experimental data adjustment, the determination of the droplets mean velocities and their adjustment to distribution functions and the determination of the dependence of the droplets velocities with the gas velocity and his properties. Finally, a section containing the final remarks and further work has been included.

VELOCITY OF THE ENTRAINED DROPLETS

The velocity profile of the entrained droplets is a key parameter to characterize the submerged jets. Due to the limited expressions specifically developed for submerged jets, in this section we will show other possible ways to estimate this droplet velocity profiles.

As it has been told above, there are very few data of the entrained droplet velocity profiles within the gas core. Few years ago, Someya et al. [2] observed that the entrained droplets travel between 1/30-1/60 of the submerged gaseous jet velocity. They proposed the next expression to determine the droplet velocity:

$$u_d = 1.08\,p_0 + 3.35 \tag{1}$$

being p_0 the stagnation pressure (given in MPa), in their experiments varies from 0.5 to 8 MPa, and the mean droplet velocity is done in m/s.

A very recent work proposes the following correlation for the determination of the entrained droplet velocity. This correlation uses the wave frequency of the gas-liquid interface (wave celerity, c), added to a percentage of the gas velocity to estimate the entrained droplet velocities [4]. The expression is as follows

$$u_d = c + 0.15 \cdot u_g \tag{2}$$

being c the wave celerity (velocity at which the waves present on the gas-liquid interface are travelling), defined as suggested by Kumar [5]

$$c = \frac{\psi \cdot J_g + J_l}{1+\psi} \tag{3}$$

and the parameter ψ is

$$\psi = 5.5\sqrt{\frac{\rho_g}{\rho_l}}\left(\frac{\mathrm{Re}_l}{\mathrm{Re}_g}\right)^{0.25} \tag{4}$$

This correlation provides predictions for the droplet velocities of 1/5 of the gas velocity, i.e., much higher velocities than those predicted by Someya's correlation.

Whereas other correlations found in the open literature, even though they were developed for fully developed annular flows, assume that droplet velocities are even higher, being between 0.5 – 0.8 of gas velocity [6,7].

Finally another way to estimate the entrained droplet velocities is via the Stokes number. This dimensionless number is defined as the ratio of the particle momentum response time (in our case the droplet response time, τ_d) over the flow system time (τ_g) [8]. Being expressed as

$$Stk = \frac{\tau_d}{\tau_g} = \frac{\rho_d \phi_d^2 u_g}{18 \mu_g D} \tag{5}$$

where D is the problem characteristic length (in our case the jet diameter). The entrained droplet behavior can be classified depending on the Stokes number values: if Stk << 1, droplets response time is almost instantaneous to any change in the gas hydrodynamics; if Stk >> 1, droplets are hardly affected by changes in the submerged gas velocity. When the Stokes number is ≈ 1, both phases have similar reaction time to any condition fluctuation. Then, by introducing the slip ratio ($S_R = u_d / u_g$), the droplet motion equations can be eventually written in terms of S_R and Stk (carrier gas acceleration, du_g/dt, assumed to be approximated as u_g/τ_g), as noted by several authors [8]:

$$S_R = \frac{u_d}{u_g} \approx \frac{1}{1+Stk} \tag{6}$$

This expression provides results, as told above, that are strongly affected mainly by the carrier gas velocity and the size distribution of the entrained droplets.

EXPERIMENTAL FACILITY, INSTRUMENTATION AND IMAGE ANALYSIS

This section aims to describe in detail the experimental facility used for the current experiment and the instrumentation techniques that were used. This setup is made to investigate the velocity profiles of the entrained droplets of a submerged gas jet injected horizontally in stagnant water pool.

Description of the Experimental Facility

The present experimental facility set up for the study of submerged gaseous jets consist of three main parts, these are: the water tank, the air injector (straight tube) and the compressed air equipment. Figure 1 illustrates the general layout of the experimental setup for the submerged gas jet injected horizontally in stagnant water. In all cases dried filtered air was used as the working fluid and treated water was used as the stagnant ambient fluid.

The tank sidewalls were made of methacrylate in order to allow the jet visualization and image film. The upper part of the tank was opened, under atmospheric pressure conditions and the bottom part of the tank features a drainage. During the experiment the tank was filled with water 30 cm above the injector level at ambient temperature. The injector was 20 cm above the tank bottom, in order to allow the free jet entry, ensuring the minimum boundary tank effects.

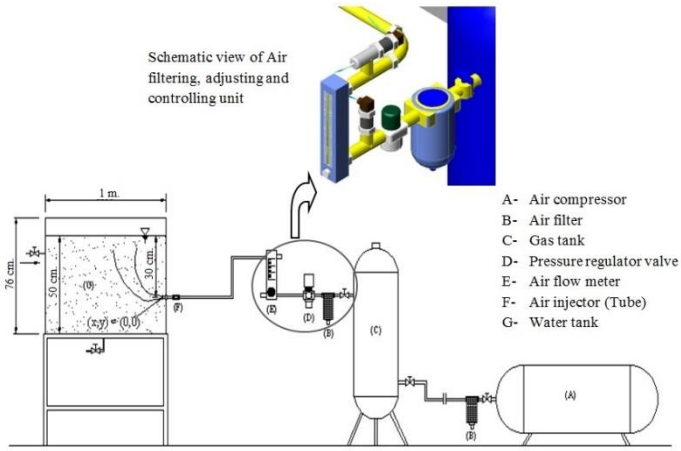

Figure 1 Schematic view of the experimental setup of the submerged jet discharge in a stagnant water pool

Instrumentation, Measurements and Image Collection

The experimental data measurements were carried out to investigate the entrained droplets of a submerged gaseous jet in a stagnant water tank under ambient conditions. Each one of the data series were collected at equilibrium conditions, that is, constant gas injection and ambient conditions.

The air mass flow rate was delivered from a central air reservoir to the water tank, so that a constant air supply is ensured. The volumetric flow rate of the air was measured using a rotameter (Key Instruments series FR 4500 with an accuracy of ±3% of full scale). The pressure of the injected air was measured using a manometer, placed near the nozzle exit. So as the jet injection velocity can be calculated.

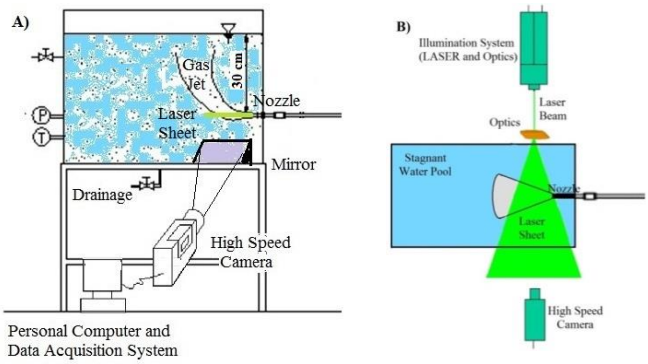

Figure 2 Schematic view of the experimental facility layout for the data acquisition system: A) Frontal View; B) Top View

The experimental setup to take the images was the following (Figure 2):

- A laser sheet intersects axially, in the horizontal axis, the gas jet, this laser sheet extends from the nozzle exit up to 5 cm long approximately.
- Because the camera cannot be found on the same plane as the laser sheet (inability to take pictures with the laser shining directly into this). Therefore, it has been needed to lower the position of the camera.
- To solve this problem, a mirror at 45 degrees has been placed on the bottom of the pool. So that the illuminated part of the jet is reflected in the mirror. While the camera is photographing the images of the jet reflected in the mirror.

Five experimental conditions were carried out, three series of 8192 images for each of them were taken (at 8000 fps, take an image every $1.25 \cdot 10^{-4}$ s).

Image Treatment and Analysis

After the image collection, they have been converted into binary images. Thus, by analyzing two consecutive images, the variation in the position of the droplets carried by the gas jet can be determined. As it has been told earlier, the water droplets were marked with fluorescent polymer microspheres to be able to see them when they were travelling into the submerged jet.

This droplet velocity detection has been done via a program of particle image velocimetry, in particular the MPIV program, which was developed by Mori and Chang [9]. This program analyzes pairs of images, giving as a result their change in position. The minimum quadric differences (MQD) algorithm has been the selected to calculate the distance between a pair of images, this algorithm is described in depth in Gui's paper [10]. This detection software has been encapsulated into a MatLab subroutine. The way in which this subroutine analyses the images is as follows: first two consecutive images are selected; after this the subroutine turns them into binary images (only white or black, with the white light areas), through the implementation of a cut-off value (the best cut-off value has been determined via a previous image analysis); then the areas that are too small are eliminated; the next step is the use of the PIV software, from him the difference in the bright points position is determined (a study of the better values required for

this program have been carried out); finally, after this, the change in position (pixel count) between the two consecutive images in both the X axis and the Y is stored in an Excel file.

After having treated all the images of an experimental data set, the next step is to determine which of them correspond to true displacements of entrained droplets, this has been done via visualization of the binary images and selecting in the Excel file the velocities higher than a critical value. This has been done in this way because there are many experimental data derived from tracer particles that are into the water pool (in the vicinity of the gas jet).This cut-off critical value is estimated from the liquid velocity near the gas-liquid interface, which will be determined with Eqn. (12).

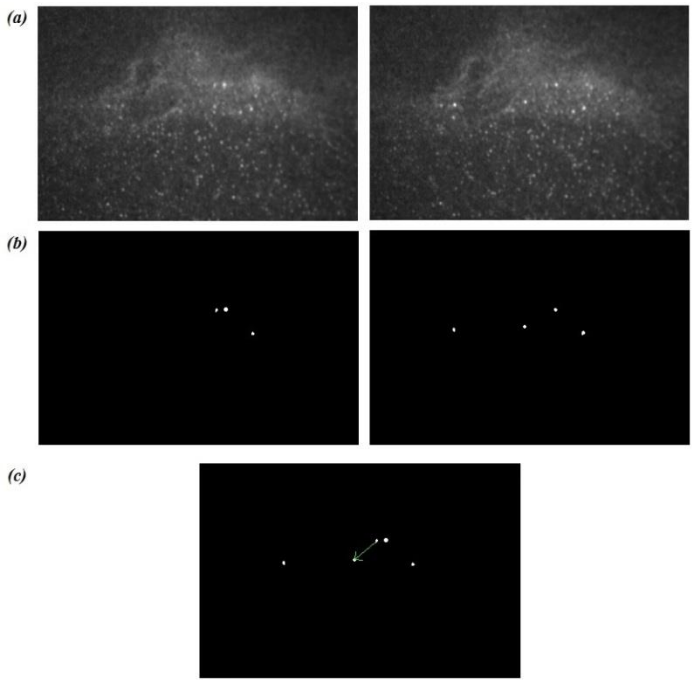

Figure 3 Image processing: (a) Images Collected by the High Speed Camera; (b)Binarization and Filtration of Images; (c) Image Treatment with PIV Toolbox

Figure 3 shows an example of processing of two consecutive images collected by the high speed camera. First the original images are binarized, the bright spots become white areas (determination of a threshold value above which white areas are considered, this value was obtained from the observation of the original images) while the rest of areas remain in black. Once the images are binarized, it has proceeded to the image treatment with a PIV program (MPIV version 0.97, [9]), a minimum quadratic differences (MQD) algorithm has been used to determine the differences in position between points to successive images. Thereby determining the velocity vector, since the position of two bright areas between two consecutive images is known. Throughout this process the velocity vectors lacking a physical sense have been removed, considering only displacements in the flow direction or with certain component in the perpendicular direction.

EXPERIMENTAL DATA AND DETERMINATION OF THE ENTRAINED DROPLET VELOCITY

The Experimental Data

A summary of the main experimental conditions, the gas velocity and the calculations of the droplets velocities for each of the five experimental data points are shown in Table 1.

The injection pressure and the gas mass flow rate were directly measured. The determination of the gas velocity was done from these two variables. Whereas the mean of the velocity for the entrained droplets have been obtained from the results of the image treatments, which have been taken with a high speed camera (Fhotron FASTCAM).

Table 1 Summary of the main experimental data measurements

	P1	P2	P3	P4	P5
Injection Pressure (MPa)	0.12	0.17	0.22	0.27	0.32
Mass Flow Rate (l/min)	35	40	45	47.5	50
v_g (m/s)	189.0	215.7	242.6	255.1	269.4
v_d (m/s)	17.16	19.82	21.38	21.80	22.16

Adjustment of the Droplet Velocity Distributions

Since the values of the droplets velocities are available for each one of the data series, it has been decided to group them into velocity ranges and make an adjustment. With this purpose, we have tested different probability distributions, concluding that the exponential distribution is the one that best fits for the experimental data. The probability density function of the exponential distribution is:

$$f(v_i,\lambda) = \lambda \exp(-\lambda v_i) \quad (7)$$

being v_i each of the entrained droplet velocity intervals and the rate parameter (reciprocal of the droplets mean velocity, $\lambda = 1/v_d$). The histograms of the droplets velocities measured experimentally and their adjustments to exponential distributions for the five experimental measurement points are shown in Figure 4. Whereas in the last row of Table 1, the droplets mean velocities for the five experimental conditions are shown.

The fundamental conclusion that can be extracted, from the results of the five experimental conditions presented in Figure 4 and in Table 1, is the good fit to the exponential distributions in all cases. A displacement towards the higher velocity intervals of the probability densities for the droplet velocities with the gas injection velocity increase can be appreciated (Figure 5). This statement is also clearly shown in Table 2, increase of the droplet mean velocities with the increase in the gas injection velocity.

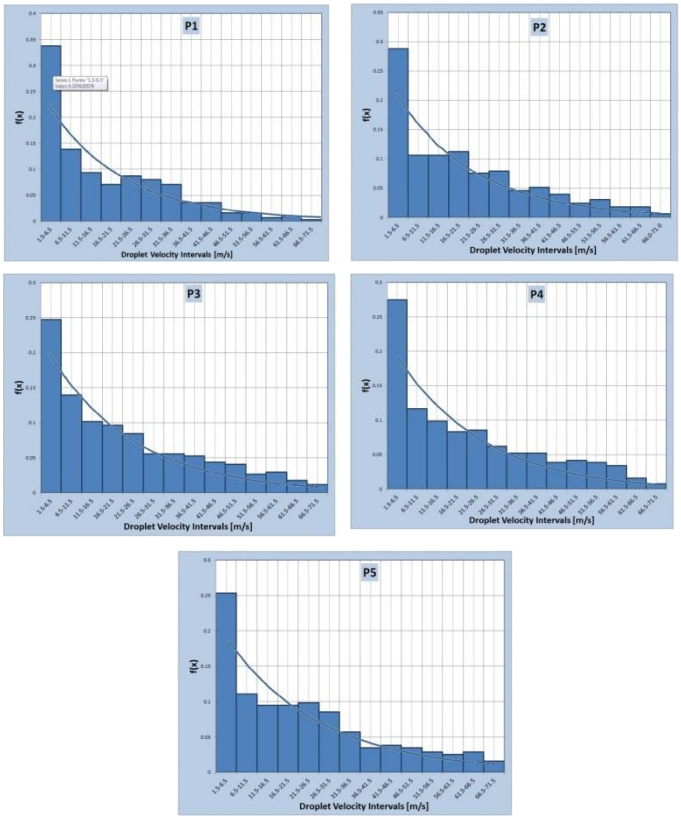

Figure 4 Adjustment of the experimental entrained droplet velocities to exponential distributions

Determination of the Droplet Sizes

Prior to setting the mean velocities of the entrained droplets with the gas injection conditions, it is necessary to proceed with the determination of the sizes of the entrained droplets. For this purpose, given the lack of expressions specifically developed for submerged jets, the correlation developed by Berna et al [11] has been employed. Although it was developed for annular flows in horizontal pipes, but this type of flows present many analogies with the submerged jets. The correlation is as follows:

$$\frac{\phi_d}{D} = 2.634 \cdot We_g^{-0.23}\, \mathrm{Re}_g^{-0.54}\, \mathrm{Re}_l^{0.13} \tag{8}$$

being We_g, Re_g and Re_l the gas Weber number and the gas and liquid Reynolds numbers respectively. They are defined as:

$$We_g = \frac{\rho_g v_g^2 D}{\sigma} \tag{9}$$

$$\mathrm{Re}_g = \frac{\rho_g v_g D}{\mu_g} \tag{10}$$

$$\mathrm{Re}_l = \frac{\rho_w v_w D}{\mu_w} \tag{11}$$

where ρ is the density and μ is the dynamic viscosity, and their subscripts g and l are referred to gas and water respectively; v_g and v_l are the gas and water velocities; σ is the water surface tension; and D is the jet diameter.

All the previously presented variables are known except the velocity of the surrounding zone to the submerged jet. The characterization of this gas-liquid interface for two fluids coming into contact sharply is very complicated, and the exact flow characteristics, at and immediately after the meeting point, of two fluids is not precisely known. But there is some basis to assume that the initial base flow is a step function of Kelvin-Helmholtz (K-H) profile. Then a base flow evolved from an initial K-H state, the stress continuity implies that [12]

$$v_w = v_g \sqrt{mr} \tag{12}$$

where m and r are the dynamic viscosity and density ratios respectively, $m = \frac{\mu_g}{\mu_w}$; $r = \frac{\rho_g}{\rho_w}$. Consequently with these last values all the calculations can be done, and the final results are shown in Figure 5.

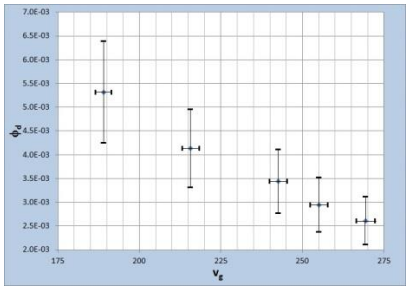

Figure 5 Determination of the entrained droplets sizes, Eqn. (8)

As it can be clearly shown watching the Eqn. (8), it can be said that the droplet sizes are strongly dependent on gas flow characteristics, being less dependent on liquid properties (higher exponent on gas Weber and Reynolds numbers than liquid Reynolds number), being an inverse dependency. An increase in gas flow rate results in a decrease in droplet sizes and vice versa, that is, exist an inverse proportionality of the entrained droplet sizes with the gas velocity. This inverse proportionality is displayed in Figure 5, in which the values of the entrained droplets sizes are drawn against the gas velocity for the five experimental conditions. With respect to errors, say that the major source of them, for both variables, comes from error propagation of the experimental measurements of the gas flow rate, reaching values around 20%.

Adjustment of the Mean Velocity of the Entrained Droplets

Many adjustments have been tested from the experimental values of the mean velocity, being finally selected a potential expression to determine the mean droplet velocity. The adjustments have been carried out with the function Robustfit of MatLab2013b, having a correlation coefficient of -0.9995 and p-values for the independent coefficient and exponent of 8.01·10-5 and 0.0027 respectively .The final expression for the droplet mean velocity is shown below:

$$\mathrm{Re}_d = 1.264 \cdot 10^7\, \mathrm{Re}_g^{-0.464} \tag{13}$$

where Re_d is the Reynolds numbers of the entrained droplets, it is defined as:

$$\mathrm{Re}_d = \frac{\rho_l v_d \phi_d}{\mu_l} \tag{14}$$

where ρ_l and μ_l are the density and dynamic viscosity of the water droplets; v_d and is the droplet velocities; and ϕ_d is the droplet mean diameter. The experimental data of the velocity measured for the entrained droplets and their adjustment to a potential function is shown in Figure 6.

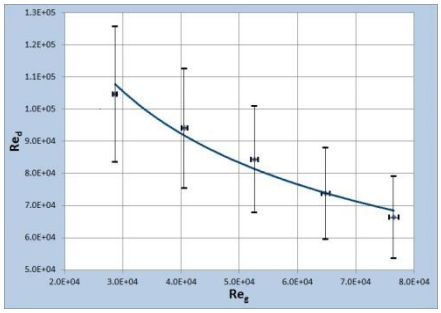

Figure 6 Adjustment of the experimental mean velocity for the entrained droplets by the submerged gas jet

The gas Reynolds number against the entrained droplet Reynolds number is presented in Figure 6, in which is clearly shown that an increase in the gas Reynolds number results in a decrease in the droplet Reynolds number and vice versa, that is, exist an inverse proportionality between these two dimensionless numbers. With regard to errors, to say that, in this case the major source of them, for both variables, also comes from error propagation of the experimental measurements of the gas flow rate, reaching values of around 20%, as in the case of the entrained droplet sizes.

FINAL REMARKS AND FURTHER WORK

As it is widely known, submerged jet hydrodynamics has an outstanding implication in many industries, such as, nuclear, metallurgical, pharmaceutical, etcetera. Throughout this document, one of the most important variables that characterizes submerged jets has been determined, the velocity at which the entrained droplets travel carried by the submerged gaseous jet. A decreasing exponential distribution function has been proved to be the one that best fits the histogram obtained from the experimental measurements of the entrained droplet velocities. In addition, one correlation which relates the submerged gas jet inlet conditions with the entrained droplets has been developed. An expression that correlates the initial submerged gaseous jets properties (done via the gas Reynolds number) with the entrained droplet mean velocity (done via the droplet Reynolds number). The use these dimensionless numbers provides a more general sense to the developed correlation, giving her greater applicability.

Concerning future works, say that the continuation of the present paper is under study. In the near future experimental measurements with other nozzle diameters will be carried out. Added to this modification, it is also intended to change the properties of the aqueous medium in which the discharge is done, this change in the aqueous properties will be carried out by the introduction of mixtures of water with other fluids.

In short, this paper is a step towards the whole knowledge of submerged gas jets injected into aqueous ponds. The velocity of the entrained droplets has been characterized, both his average value and his distribution function. Being still pending his extension to other nozzle diameters and properties of the surrounding medium, these subjects will be held in the near future.

ACKNOWLEDGMENTS

The authors are indebted to the financial support of MODEXFLAT project, reference: ENE2013-48565-C2-1-P.

REFERENCES

[1] • Hoefele, E.O. & Brimacombe, J.K., "Flow Regimes in Submerged Gas Injection". Metallurgical Transactions, Vol. 10B, 1979, pp. 631-648.

[2] • Someya, S., Uchida M, Li, Y., Ohshima, H. & Okamoto, K., "Entrained droplets in underexpanded gas jet in water". Journal of Visualization, DOI 10.1007/s12650-011-0089-7, 2011.

[3] • Roger, F., Carreau, J-L, Gbahoué, L., Hobbes, P., Allou, A. & Beauchamp, F., "Structure of strongly underexpanded gas jets submerged in liquids– Application to the wastage of tubes by aggressive jets", Nuclear Engineering and Design, Vol. 273, p.p. 119-130, 2014.

[4] Berna, C., Escrivá, A., Muñoz-Cobo, J. L. & Herranz, L.E., "Enhancement of the SPARC90 code to pool scrubbing events under jet injection regime". Nuclear Engineering and Design, accepted under review.

[5] • Mantilla I., "Mechanistic Modeling of Liquid Entrainment in Gas in Horizontal Pipes". PhD. Thesis University of Tulsa, 2008.

[6] • Fore, L. B. & Dukler, A. E., "The distribution of drop size and velocity in gas-liquid annular flow". Int. J. Multiphase Flow 21, pp. 137-149, 1995.

[7] • Azzopardi, B. J., "Drops in annular two-phase flow". International Journal of Multiphase Flow, Vol. 23, pp. 1-53., 1997.

[8] • Crowe, C.T., "Multiphase Flow Handbook (Mechanical Engineering)". CRC Press, Taylor and Francis Group, 2006.

[9] • Mori, N. & Chang, K-A., "Introduction to MPIV". Mpiv – MATLAB PIV Toolbox: http://www.oceanwave.jp/softwares/mpiv/, 2009.

[10] • Gui, L. C. & Merzkirch, W., "A method of tracking ensembles of particle images". Experiments in fluids, Vol 21, p.p. 465-468, 1996.

[11]• Berna, C., Escrivá, A., Muñoz-Cobo, J.L. & Herranz, L.E., "Review of droplet entrainment in annular flow: characterization of the entrained droplets". Progress in Nuclear. Energy, vol. 79, p.p. 64-86 (2015)..

[12] • Yecko, P., "Viscous modes in two-phase mixing layers". Physics of Fluid, Vol. 14, p.p. 4115-4121, 2002.